

Driven translocation of a flexible polymer through an interacting conical pore

Rajneesh Kumar,^{*} Abhishek Chaudhuri,[†] and Rajeev Kapri[‡]
*Indian Institute of Science Education and Research Mohali,
Knowledge City, Sector 81, S. A. S. Nagar – 140 306, Punjab India.*
(Dated: February 17, 2021)

We study the driven translocation of a flexible polymer through an interacting conical pore using Langevin dynamics simulations. We find that, for a fixed value of externally applied force and pore polymer interaction strength, the mean residence time of monomers inside the pore shows non-monotonic variations with pore apex angle α . We explain this behavior using a free energy argument by explicitly accounting for pore-polymer interactions and external drive. Our theoretical observations are corroborated by the simulation results of the mean translocation times as the pore-polymer interactions and external driving force are varied.

PACS numbers: 87.15.ap, 82.35.Lr, 82.35.Pq

Polymer translocation is a complex ubiquitous phenomena found in many biological processes like the passage of mRNA through nuclear pore complexes, protein translocation across biological membranes through a narrow channel, injection of DNA from a virus head into a host cell and gene swapping between bacteria [1, 2]. The translocation of a polymer through a narrow pore has attracted considerable attention both experimentally [3–14] and theoretically [15–50] in the last two decades due to its potential in designing inexpensive, fast and direct sequencing devices for biomolecules like DNA. Biomolecules such as DNA, moving through a narrow pore blocks the flow of ionic current through the pore. The resultant ionic current trace is expected to give information of the DNA sequence that is passing through the pore. This has led to the extensive use of both biological and synthetic nanopores as biosensors, for example in sequence detection.

Biological nanopores such as α -haemolysin [51], MspA [52–54], phi29 [55] and recently wild-type aerolysin nanopore [56] have been used to investigate both single stranded DNA (ssDNA) and double stranded DNA (dsDNA) sequencing. However, biological nanopores are known to be unstable with changes in pH, temperature and mechanical oscillations [5]. Further, the role of pore geometry in the translocation process and the ability to tune the pore geometry to provide the best sequencing platform, is difficult to address in the context of biological nanopores.

Solid state nanopores [57–62], on the other hand, have been shown to be stable with respect to reasonable changes in pH and temperature and can be fabricated to a wide range of shapes and sizes. One of the challenges of nanopore based sequencing technologies is that translocation of ssDNA through nanopores is extremely fast, the ionic current signatures of single DNA

nucleotides masked by fluctuations. Therefore sequencing techniques have focused at slowing down the transport of ssDNA before readout. In this regard, asymmetrical conical nanopores with tapering angles have great potential for sensing applications, the constricting geometry slowing down translocation of biomolecules and the tip of the cone acting like a sensing zone [5, 8]. This has led to several experimental studies of translocation of biomolecules through fabricated solid state conical nanopores [63]. Conical nanocapillaries have been used to study detection of DNA and other proteins, the conical shape of the pore resulting in ionic current rectification at low salt concentrations [63–65]. An alternative technique using glass nanocapillaries, as opposed to solid state nanopores, was capable of simultaneous ionic current and fluorescent detection of DNA translocation [66]. Even for biological nanopores such as the α -hemolysin, pore asymmetry is known to affect the capture rate and current signature of DNA depending on its direction of transport [67].

On the theoretical front, there have been only a few studies on polymer translocation through conical nanopores [68–71]. These studies have shown that the shape of the asymmetric conical channel gives rise to an effective entropic force that drives translocation and that the translocation time is a non-monotonic function of the apex angle of the pore. However, in all experimental scenarios, the translocation process is driven and the interactions of the polymer with the pore is extremely important in determining the efficiency of the translocation process. It is therefore imperative to understand the extent to which the non-monotonicity in the translocation times persists in presence of external drive and varying pore-polymer interactions. In Refs. [70, 72], ionic conductivity and polymer translocation in the presence of external driving in three different conical shaped nanopore geometries were studied. Polymer translocation was shown to be heavily dependent on the structures of the pore for different pore-polymer interactions and external voltage. However, a systematic understanding of the non-linear effects of translocation times on the pore-polymer interactions and external voltage as the angle of the conical

^{*} rajneesh@jncasr.ac.in, Present address: Theoretical Science Unit, Jawaharlal Nehru Center for Advanced Scientific Research, Jakkur, Bangalore –560064 India.

[†] abhishek@iisermohali.ac.in

[‡] rkapri@iisermohali.ac.in

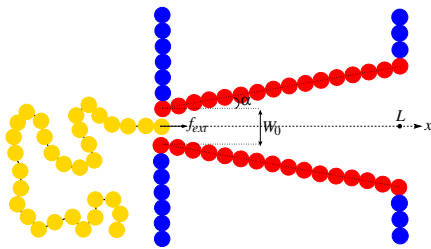


FIG. 1. Schematic diagram of a polymer translocating through a conical pore with an half apex angle α . The width (at the apex) and the length of the pore is $W_0 = 2.25\sigma$ and $L = 16\sigma$, respectively.

pore is varied, is missing.

In this paper, we study the driven translocation of a flexible polymer through an interacting conical pore with a small entry and a large exit, using Langevin dynamics simulations. We look at the mean residence time distribution $\langle r(s) \rangle$ of a monomer s inside the conical pore. The mean residence time distribution shows non-monotonic features with the tapering angle α of the pore which are distinctly different from that through a rectangular channel of same length. We show how $\langle r(s) \rangle$ can be tuned with α and the external driving force. We explain the observations using free energy arguments which includes both the entropic contributions due to confinement and the synergetics of the pore-polymer interactions. Finally we show that the non-monotonic behavior of the mean translocation time with changing apex angle, is strongly affected by both the pore-polymer interactions and the external driving force.

We model the polymer by beads and springs in two dimensions. A schematic diagram of a flexible polymer translocating from the *cis* to the *trans* side of a conical pore is shown in Fig. 1. The beads of the polymer experience an excluded volume interaction modeled by the Weeks-Chandler-Andersen (WCA) potential of the form

$$U_{\text{bead}}(r) = \begin{cases} 4\varepsilon \left[\left(\frac{\sigma}{r}\right)^{12} - \left(\frac{\sigma}{r}\right)^6 \right] + \varepsilon & \text{for } r \leq r_{\text{min}} \\ 0 & \text{for } r > r_{\text{min}} \end{cases} \quad (1)$$

where, ε is the strength of the potential. The cutoff distance, $r_{\text{min}} = 2^{1/6}\sigma$, is set at the minimum of the potential. The consecutive monomers in the chain interact via harmonic potential of the form

$$U_{\text{bond}}(r) = K(r - r_0)^2, \quad (2)$$

where K is the spring constant and r_0 is the equilibrium separation between consecutive monomers of the chain.

The pore and walls are made from stationary monomers separated by a distance of σ from each other. The conical pore is made up of two rows of monomers symmetric about the x -axis with an apex angle $\theta = 2\alpha$. The length of the pore is taken to be $L = 16\sigma$ with a width $W_0 = 2.25\sigma$ at the apex. This pore width allows only single-file entrance of the polymer and avoid

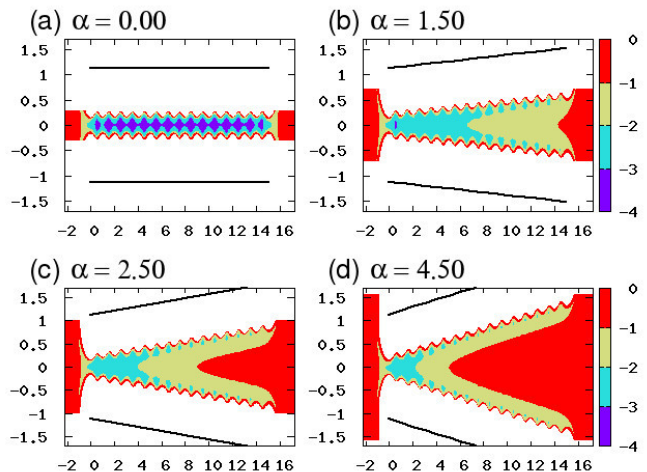


FIG. 2. Potential energy landscape for various pore apex angles $\alpha = 0, 0.25, 1.5$ and 4.5 used in our simulations. Potential depth increases from red to purple.

the formation of hairpin configurations at the apex opening [45–47]. The interaction of the pore with the polymer is chosen to be the standard LJ form:

$$U_{\text{pore}}(r) = \begin{cases} 4\varepsilon_p \left[\left(\frac{\sigma}{r}\right)^{12} - \left(\frac{\sigma}{r}\right)^6 \right] & \text{for } r \leq r_c \\ 0 & \text{for } r > r_c, \end{cases} \quad (3)$$

where ε_p denotes the potential depth and $r_c = 2.5\sigma$ is the cutoff distance. The interaction of polymer with walls, U_{wall} , is modeled by WCA potential given by Eq. (1). The potential energy landscape inside the pore for various pore angles are shown in Fig. 2. For small apex angles, there is a strong attraction near the *cis* side of the pore and a strong barrier near the *trans* side. As the apex angle increases, the barrier near the *trans* side shifts toward the *cis* side of the pore.

The polymer experiences a driving force, $\mathbf{f}_{\text{ext}} = f\hat{x}$ directed along the pore axis with magnitude f , which mimics the electrophoretic driving of biopolymers through nanopores. To initiate the translocation process, we start with a chain configuration with the first bead placed at the entrance of the pore. This bead is fixed and the remaining beads are allowed to fluctuate so that the chain can relax to its equilibrium configuration. The first bead is then released and the translocation of the polymer across the pore is monitored. The translocation time τ is defined as time elapsed between the entrance of the first bead of the polymer and the exit of all the beads from the channel. We discard all failed translocation events.

To integrate the equation of motion for the monomers of the chain we use Langevin dynamics algorithm with velocity Verlet update. The equation of motion for a monomer is given by

$$m\ddot{\mathbf{r}}_i = -\nabla U_i + \mathbf{f}_{\text{ext}} - \zeta\mathbf{v}_i + \boldsymbol{\eta}_i, \quad (4)$$

where m is the monomer mass, $U_i = U_{\text{bond}} + U_{\text{bead}} + U_{\text{wall}} + U_{\text{pore}}$ is the total potential experienced by

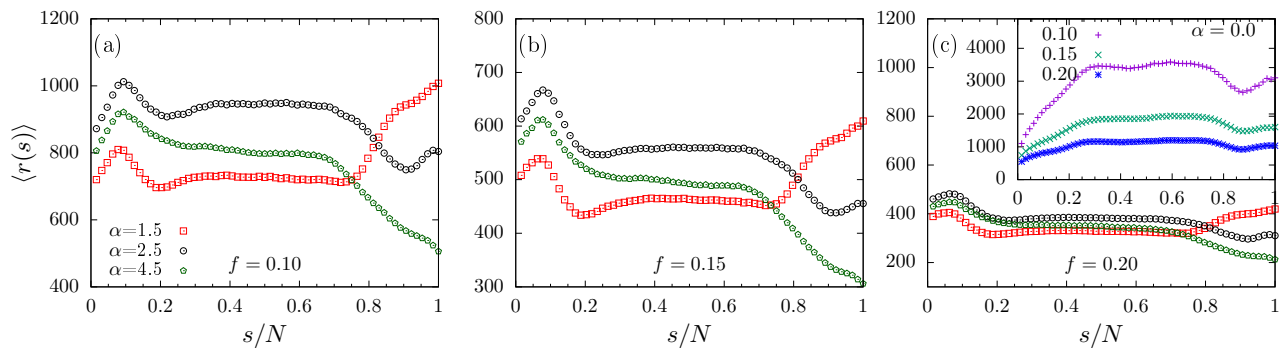


FIG. 3. The mean residence time $\langle r(s) \rangle$, for a flexible polymer of length $N = 64$ as a function of s/N for various pore half-apex angles α for external driving forces (a) $f = 0.1$, (b) $f = 0.15$, and (c) $f = 0.2$. The strength of pore-monomer interaction is $\epsilon_p = 0.9$. The inset shows the mean residence time for half-apex angle $\alpha = 0$ for various values of driving forces.

i th monomer, ζ is the friction coefficient, \mathbf{v}_i is the monomer's velocity, and $\boldsymbol{\eta}_i$ is the random force satisfying the fluctuation-dissipation theorem $\langle \eta_i(t) \eta_j(t') \rangle = 2\zeta k_B T \delta_{ij} \delta(t - t')$. The unit of energy, length and mass are set by ϵ , σ , and m , respectively, which sets the unit of time as $\sqrt{m\sigma^2/\epsilon}$. In these units, we choose $\zeta = 1.0$, $K = 10^3 k_B T / \sigma$, $r_0 = 1.12\sigma$ and $k_B T = 1.0$, and the number of polymer beads $N = 64$ in our simulations. A time step of $\Delta t = 0.005$ is used in all simulation runs.

We first look at the mean residence time, $\langle r(s) \rangle$, of a monomer s inside the pore. It is defined as the total time spent by the monomer s inside the pore between its entrance at the pore apex and its first exit from the base of the conical pore. In Fig. 3, $\langle r(s) \rangle$ is plotted as a function of monomer index s for a polymer of length $N = 64$ for different values of pore half-apex angles α , and various external driving forces f for a fixed pore-polymer interaction strength, ϵ_p .

We first look at $\alpha = 0$, i.e a flat pore. As seen in Fig. 3(c, inset), for small driving forces, $\langle r(s) \rangle$ increases with s for the initial monomers, then saturates and finally shows a non-monotonic variation for the end monomers of the chain. This behavior can be explained using the tension propagation theory [26, 31–33, 36–42] with pore-polymer interactions. The part of the polymer on the *cis*-side is divided into two distinct domains. The external driving force and the attractive interactions of the pore with the polymer, pulls on the monomers nearer to the pore and sets them in motion. The remaining monomers that are farther away from the pore, do not experience the pull and on average remain at rest. As the polymer gets sucked inside, more and more monomers on the *cis* side start responding to the force, with a tension front separating the two domains propagating along the length of the polymer. The time dependent drag experienced by a monomer $\zeta(t)$ increases as the tension front propagates and more number of monomers on the *cis* side get involved. This increase in the effective friction is manifested in the residence times which show an initial increase with s , implying that subsequent monomers spends more time inside the pore. This continues until

$\zeta(t)$ becomes maximum when the tension front reaches the last monomer, maximum number of monomers at the *cis*-side participating in the translocation process. Beyond this, the system enters the tail retraction stage where the monomers on the *cis* side starts decreasing and therefore $\zeta(t)$ decreases and so does the waiting time $\langle r(s) \rangle$. For the end monomers exiting the extended pore, the effect of the attractive interactions of the pore become more dominant compared to entropic effects which increases their residence time inside the pore. As the external driving force increases, this increase in $\langle r(s) \rangle$ for the end monomers is minimal.

As α increases, we observed several interesting effects which can be attributed to the conical nature of the pore. For non-zero α , $\langle r(s) \rangle$ shows a hump for the initial monomers. The initial increase follows from the argument of tension propagation theory as stated above. The decrease in $\langle r(s) \rangle$ observed before the saturation region is a result of the entropic gain as the initial monomers move into a larger region than that of a flat pore. The effective drag reduces leading to a lowering of $\langle r(s) \rangle$. The saturation regime follows as the tension propagates to the end monomers. The dominant effect of the pore-polymer interactions on the end monomers which results in an increase in $\langle r(s) \rangle$, reduces as α increases. Further note that $\langle r(s) \rangle$ is lowest for all s (except for the end monomers) for $\alpha = 1.5$, increases for $\alpha = 2.5$ and decreases for $\alpha = 4.5$. This indicates a non-monotonic dependence of the total translocation time with α consistent with earlier observations. For increasing driving forces, the subtle competition between entropy and pore synergetics decreases and the features in $\langle r(s) \rangle$ are less pronounced.

We now provide a theoretical description of the translocation process using a free energy argument. We need to estimate the free-energy change due to the confinement, F_c , of the polymer inside the conical channel. Let us consider a partly confined chain in the channel in the presence of an external driving force \mathbf{f}_{ext} . The confinement of the polymer inside the pore costs entropy. We assume that the part of the polymer chain that is inside the pore breaks up into blobs of size $\xi(x) = W_0 \cos \alpha + 2x \sin \alpha$ that

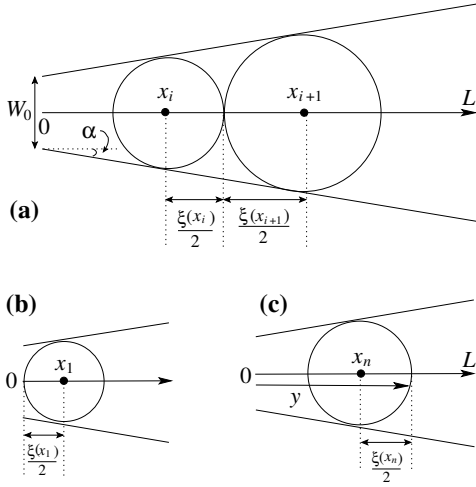


FIG. 4. (a) Two consecutive blobs inside the conical pore. The diameter $\xi(x_i)$ of a blob depends on the position x_i along the pore axis. This figure also shows the relation satisfied by two consecutive blobs. (b) The location of the first blob is tangent to the beginning of the conical pore. (c) The location of the n th blob is at a distance y from the entrance of the conical pore.

are tangent to the pore walls as shown in Fig 3. Then, the entropic penalty due to the confinement of chain in the conical channel is of the order of $k_B T$ per blob. If $N_b(y)$ represents the number of blobs that penetrate a distance y into the channel, we have $F_c(y) \sim k_B T N_b(y)$.

To count $N_b(y)$, we consider two consecutive blobs inside the conical pore at positions x_j and x_{j+1} with diameters $\xi(x_j)$ and $\xi(x_{j+1})$, respectively as shown in Fig. 4. They satisfy the relation

$$x_{j+1} = x_j + \frac{1}{2} [\xi(x_j) + \xi(x_{j+1})]. \quad (5)$$

Using this recursion relation, one can easily obtain an expression between the position of the blob x_j and its number j along the pore [68] as

$$x_j = \mathcal{Q}^{j-1} \left(x_1 + \frac{W_0}{2 \tan \alpha} \right) - \frac{W_0}{2 \tan \alpha}, \quad (6)$$

where $\mathcal{Q} = (1 + \sin \alpha)/(1 - \sin \alpha)$. The first blob is tangent to the beginning of the pore and its location along the axis is given by $x_1 = \xi(x_1)/2$. The last (say n th) blob is tangent to the pore at a distance y from the pore entrance, hence its location x_n along the axis is given by $x_n = y - \xi(x_n)/2$. The blob number n , and hence $N_b(y)$, can be obtained by Using Eq. (6) along with x_1 and x_n , and hence the free-energy cost due to the confinement as a function of distance y along the pore axis is given by

$$\frac{F_c(y)}{k_B T} \sim N_b(y) \sim \frac{\log \mathcal{P}}{\log \mathcal{Q}}, \quad (7)$$

where $\mathcal{P} = 1 + 2y \tan \alpha / W_0$.

The second contribution to the free-energy is due to the constant external force, f , experienced by the segment of the polymer which is inside the pore, denoted by F_f . The value of F_f changes with the number of monomers which are present inside the pore. The free energy change corresponds to the work done to displace the chain by a distance y inside the pore and is given by

$$\begin{aligned} \frac{F_f(y)}{k_B T} &\sim - \int_0^y f N_b(x) dx \\ &\sim - \frac{f}{2 \log \mathcal{Q}} \left[2y - \left(2y + \frac{W_0}{\tan \alpha} \right) \log \mathcal{P} \right], \quad (8) \end{aligned}$$

where f is the magnitude of the external force f_{ext} acting inside the pore towards the trans direction.

The final contribution to the free-energy is due to the attractive interactions with the walls of the channel. We need to determine the number of monomers in the blobs that are in contact with two walls of the conical channel. In 2D, the number of monomers in j th blob is given by $m(x_j) = (\xi(x_j)/\sigma)^{4/3}$. The total number of monomers N_n in n blobs up to the distance y inside the channel can then be obtained from the constraint $N_n(y) = \sum_{j=1}^n m(x_j)$. Substituting x_j from the recursion relation Eq. (6), and number of blobs $N_b(y)$, we get

$$N_n(y) = \sigma^{-\frac{4}{3}} \frac{(2y \sin \alpha + W_0 \cos \alpha)^{\frac{4}{3}} - (W_0 \cos \alpha)^{\frac{4}{3}}}{(1 + \sin \alpha)^{\frac{4}{3}} - (1 - \sin \alpha)^{\frac{4}{3}}}. \quad (9)$$

The fraction of monomers that are in contact with a wall of the channel is then given by $N_n(y)(\sigma/\xi(y))$. If $V(y)$ denotes the interaction energy, which is due to the pore-polymer interaction and given by the LJ potential (Eq. (3)), the free energy contribution due to the attractive interaction for a polymer that has entered the pore up to a distance y is given by

$$\frac{F_p(y)}{k_B T} \sim V(y) N_n(y) \left(\frac{\sigma}{\xi(y)} \right). \quad (10)$$

The total free energy is then given by

$$\frac{F_{tot}(y)}{k_B T} = \frac{1}{k_B T} (F_f(y) + A F_p(y) + C F_c(y)), \quad (11)$$

where A and C are undetermined factors.

In Fig. 5, we have plotted the total free energy $F_{tot}/k_B T$, given by Eq. (11), for parameter values $A = 0.035$ and $C = 1$, as a function of distance y along the pore axis for different half-apex angle α ranging from $\alpha = 0.5^\circ$ to $\alpha = 5^\circ$ for a polymer of length $N = 64$ with an external force $f = 0.1$ and pore polymer interaction energy strength $\varepsilon_p = 1$. The free energy exhibits a barrier that needs to be overcome by the polymer to translocate towards the trans side successfully. As α increases, the barrier height also increases indicating that it is relatively more difficult for the polymer to translocate towards the trans end. The free energy barrier attains a maximum height at $\alpha = 2^\circ$ and on increasing α further,

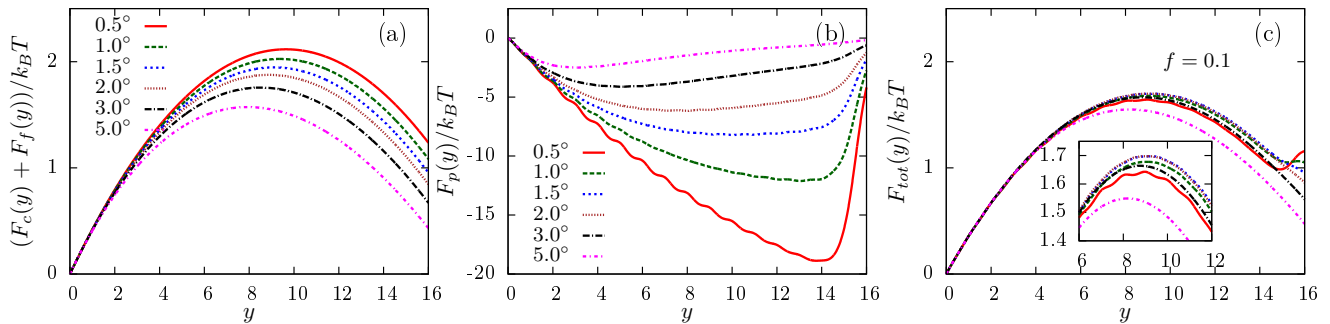


FIG. 5. (Color online) (a) Sum of free energy contributions due to confinement and external force $(F_c + F_f)/k_B T$, (b) Free energy due to pore interaction $F_p/k_B T$, (c) Total free energy $F_{tot}/k_B T$, as a function of distance y from the pore apex along the pore axis for different half-apex angle α for a polymer of length $N = 64$ with an external force $f = 0.1$. The inset shows the data near the peak region.

the barrier starts decreasing showing that polymer can easily translocate from the conical pore for larger apex angle. This explains the non-monotonic dependence of residence times and average translocation times on the pore angle.

In the above analysis, we have taken the interaction energy, which comes due to pore-polymer interactions, to be one-dimensional. However, the actual interaction energy is two-dimensional. The potential energy landscape presented in Fig. 2, clearly indicate that for very small values of α , the position of the potential barrier is nearer to the trans side of pore, which corroborates the free energy picture. So for small apex angles, the translocation process is an interplay between confinement effects and interactions of the polymer with the pore. But as the α increases, position of the potential barrier start moving towards the apex of the pore as can be seen from the red region moving close to the pore entry. As the driving force is increased, the translocation is faster. The polymer will take less time to overcome the barrier as compared to the smaller values of driving forces. At sufficiently strong driving force, effect of pore-polymer interaction becomes negligible and translocation time is expected to decrease monotonically with the apex angle of the pore (Fig. 2).

In Fig. 6(a), we plot the variation of mean translocation time $\langle \tau \rangle$ as a function of α for different strengths of pore-polymer interaction, ε_p , at a fixed value of the external force $f = 0.1$. As is evident from the free energy argument, F_p dominates the translocation process as ε_p increases. With increasing ε_p , the free energy barrier near the exit of the pore is high and the polymer spends longer time inside the pore and therefore, $\langle \tau \rangle$ increases with ε_p for all values of α . With increasing α since the barrier falls drastically, the translocation times are significantly less. However, the non-monotonic feature persists even for driven translocation with the hump observed near $\alpha \approx 2^\circ$. In Fig. 6(b), we observe that with increasing external drive f at a fixed ε_p , the mean translocation time $\langle \tau \rangle$ decreases for all α . The non-monotonic feature starts disappearing at higher f .

We have studied the driven translocation of a flexible polymer through an interacting cone shaped pore. Conical nanopores have several advantages in bio-sensing applications and the influence on translocation behavior of the interactions with the surface of the pore and the external drive are of significant interest. Using free energy arguments, we have shown that non-monotonic features in translocation times observed in conical pores persist

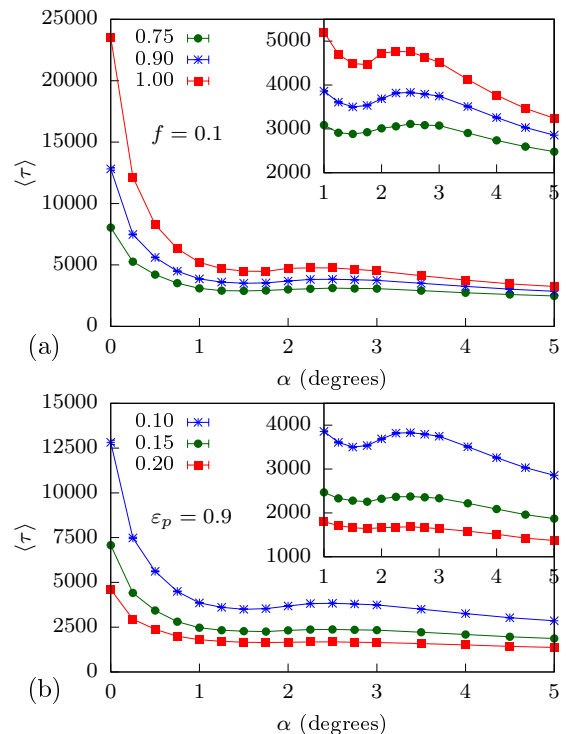


FIG. 6. (a) Average translocation time $\langle \tau \rangle$ as a function of pore apex angle α : (a) For various strength of pore-polymer interaction ε_p at pulling force $f = 0.1$. (b) For various pulling forces f by keeping $\varepsilon_p = 0.9$. The length of the polymer is $N = 64$.

even in the presence of the experimentally relevant scenarios of driven translocation with pore-polymer interactions. Extensive Langevin dynamics simulations confirm these observations. The mean residence times also show behaviors characteristic of translocation through conical

pores. Their behavior with changing external drive is consistent with tension propagation along the polymer backbone. The mean translocation time $\langle\tau\rangle$ is found to be strongly dependent on the strength of pore-polymer interaction and the external driving force.

-
- [1] M. Muthukumar, *Polymer translocation* (CRC press, 2016).
- [2] V. V. Palyulin, T. Ala-Nissila, and R. Metzler, *Soft matter* **10**, 9016 (2014).
- [3] D. Branton, D. W. , A. Marziali, H. Bayley, S. A. Benner, T. Butler, M. Di Ventra, S. Garaj, A. Hibbs, X. Huang, *et al.*, in *Nanoscience and technology: A collection of reviews from Nature Journals* (World Scientific, 2010) pp. 261–268.
- [4] M. Wanunu, *Physics of life reviews* **9**, 125 (2012).
- [5] S. Howorka and Z. Siwy, *Chemical Society Reviews* **38**, 2360 (2009).
- [6] D. Deamer, M. Akeson, and D. Branton, *Nature biotechnology* **34**, 518 (2016).
- [7] C. A. Merchant, K. Healy, M. Wanunu, V. Ray, N. Peterman, J. Bartel, M. D. Fischbein, K. Venta, Z. Luo, A. C. Johnson, *et al.*, *Nano letters* **10**, 2915 (2010).
- [8] U. F. Keyser, *Journal of The Royal Society Interface* **8**, 1369 (2011).
- [9] L.-Q. Gu, M. Wanunu, M. X. Wang, L. McReynolds, and Y. Wang, *Expert review of molecular diagnostics* **12**, 573 (2012).
- [10] B. M. Venkatesan and R. Bashir, *Nature nanotechnology* **6**, 615 (2011).
- [11] A. Meller, *Journal of physics: condensed matter* **15**, R581 (2003).
- [12] L. Movileanu, *Soft Matter* **4**, 925 (2008).
- [13] L. Movileanu, *Trends in Biotechnology* **27**, 333 (2009).
- [14] S. Majd, E. C. Yusko, Y. N. Billeh, M. X. Macrae, J. Yang, and M. Mayer, *Current Opinion in Biotechnology* **21**, 439 (2010).
- [15] A. Aksimentiev, *Nanoscale* **2**, 468 (2010).
- [16] A. Milchev, *Journal of Physics: Condensed Matter* **23**, 103101 (2011).
- [17] D. Panja, G. T. Barkema, and A. B. Kolomeisky, *Journal of Physics: Condensed Matter* **25**, 413101 (2013).
- [18] W. Sung and P. Park, *Physical review letters* **77**, 783 (1996).
- [19] D. K. Lubensky and D. R. Nelson, *Biophysical journal* **77**, 1824 (1999).
- [20] M. Muthukumar, *The Journal of Chemical Physics* **111**, 10371 (1999).
- [21] M. Muthukumar and C. Kong, *Proceedings of the National Academy of Sciences* **103**, 5273 (2006).
- [22] M. Muthukumar, *The Journal of chemical physics* **132**, 05B605 (2010).
- [23] C. T. A. Wong and M. Muthukumar, *The Journal of chemical physics* **133**, 07B607 (2010).
- [24] M. Muthukumar, *Physical Review Letters* **86**, 3188 (2001).
- [25] C. Kong and M. Muthukumar, *The Journal of chemical physics* **120**, 3460 (2004).
- [26] T. Sakaue, *Physical Review E* **76**, 021803 (2007).
- [27] D. Panja, G. T. Barkema, and R. C. Ball, *Journal of Physics: Condensed Matter* **19**, 432202 (2007).
- [28] J. Dubbeldam, A. Milchev, V. Rostiashvili, and T. A. Vilgis, *EPL (Europhysics Letters)* **79**, 18002 (2007).
- [29] M. G. Gauthier and G. W. Slater, *The Journal of chemical physics* **128**, 02B612 (2008).
- [30] M. G. Gauthier and G. W. Slater, *The Journal of Chemical Physics* **128**, 05B619 (2008).
- [31] T. Saito and T. Sakaue, *The European Physical Journal E* **34**, 135 (2011).
- [32] T. Saito and T. Sakaue, *Physical Review E* **85**, 061803 (2012).
- [33] T. Sakaue, *Polymers* **8**, 424 (2016).
- [34] R. Ledesma-Aguilar, T. Sakaue, and J. M. Yeomans, *Soft Matter* **8**, 1884 (2012).
- [35] L. Liu, C. Yang, K. Zhao, J. Li, and H.-C. Wu, *Nature communications* **4**, 1 (2013).
- [36] P. Rowghanian and A. Y. Grosberg, *The Journal of Physical Chemistry B* **115**, 14127 (2011).
- [37] T. Ikonen, A. Bhattacharya, T. Ala-Nissila, and W. Sung, *Physical Review E* **85**, 051803 (2012).
- [38] T. Ikonen, A. Bhattacharya, T. Ala-Nissila, and W. Sung, *The Journal of chemical physics* **137**, 085101 (2012).
- [39] T. Ikonen, A. Bhattacharya, T. Ala-Nissila, and W. Sung, *EPL (Europhysics Letters)* **103**, 38001 (2013).
- [40] J. Sarabadani, T. Ikonen, and T. Ala-Nissila, *The Journal of Chemical Physics* **141**, 214907 (2014).
- [41] J. Sarabadani, T. Ikonen, H. Mökkönen, T. Ala-Nissila, S. Carson, and M. Wanunu, *Scientific reports* **7**, 1 (2017).
- [42] J. Sarabadani and T. Ala-Nissila, *Journal of Physics: Condensed Matter* **30**, 274002 (2018).
- [43] B. Ghosh, J. Sarabadani, S. Chaudhury, and T. Ala-Nissila, *Journal of Physics: Condensed Matter* **33**, 015101 (2020).
- [44] S. Buyukdagli, J. Sarabadani, and T. Ala-Nissila, *Polymers* **11**, 118 (2019).
- [45] J. A. Cohen, A. Chaudhuri, and R. Golestanian, *Physical review letters* **107**, 238102 (2011).
- [46] J. A. Cohen, A. Chaudhuri, and R. Golestanian, *Physical Review X* **2**, 021002 (2012).
- [47] J. A. Cohen, A. Chaudhuri, and R. Golestanian, *The Journal of chemical physics* **137**, 204911 (2012).
- [48] K. Luo, T. Ala-Nissila, S.-C. Ying, and A. Bhattacharya, *Physical Review Letters* **99**, 148102 (2007).
- [49] K. Luo, T. Ala-Nissila, S.-C. Ying, and A. Bhattacharya, *Physical Review Letters* **100**, 058101 (2008).
- [50] R. Kumar, A. Chaudhuri, and R. Kapri, *The Journal of chemical physics* **148**, 164901 (2018).
- [51] J. J. Kasianowicz, E. Brandin, D. Branton, and D. W. Deamer, *Proceedings of the National Academy of Sciences* **93**, 13770 (1996).
- [52] I. M. Derrington, T. Z. Butler, M. D. Collins, E. Manrao, M. Pavlenok, M. Niederweis, and J. H. Gundlach, *Proceedings of the National Academy of Sciences* **107**,

- 16060 (2010).
- [53] T. Z. Butler, M. Pavlenok, I. M. Derrington, M. Niederweis, and J. H. Gundlach, *Proceedings of the National Academy of Sciences* **105**, 20647 (2008).
- [54] E. A. Manrao, I. M. Derrington, A. H. Laszlo, K. W. Langford, M. K. Hopper, N. Gillgren, M. Pavlenok, M. Niederweis, and J. H. Gundlach, *Nature biotechnology* **30**, 349 (2012).
- [55] D. Wendell, P. Jing, J. Geng, V. Subramaniam, T. J. Lee, C. Montemagno, and P. Guo, *Nature nanotechnology* **4**, 765 (2009).
- [56] C. Cao, Y.-L. Ying, Z.-L. Hu, D.-F. Liao, H. Tian, and Y.-T. Long, *Nature Nanotechnology* **11**, 713 (2016).
- [57] C. Dekker, *Nature nanotechnology* **2**, 209 (2007).
- [58] M. Wanunu and A. Meller, *Nano letters* **7**, 1580 (2007).
- [59] M. Gershow and J. A. Golovchenko, *Nature nanotechnology* **2**, 775 (2007).
- [60] F. Haque, J. Li, H.-C. Wu, X.-J. Liang, and P. Guo, *Nano today* **8**, 56 (2013).
- [61] B. Luan, G. Stolovitzky, and G. Martyna, *Nanoscale* **4**, 1068 (2012).
- [62] U. F. Keyser, B. N. Koeleman, S. Van Dorp, D. Krapf, R. M. Smeets, S. G. Lemay, N. H. Dekker, and C. Dekker, *Nature Physics* **2**, 473 (2006).
- [63] J. Zhou, Y. Wang, L. D. Menard, S. Panyukov, M. Rubinstein, and J. M. Ramsey, *Nature communications* **8**, 1 (2017).
- [64] C. C. Harrell, Y. Choi, L. P. Horne, L. A. Baker, Z. S. Siwy, and C. R. Martin, *Langmuir* **22**, 10837 (2006).
- [65] W.-J. Lan, D. A. Holden, and H. S. White, *Journal of the American Chemical Society* **133**, 13300 (2011).
- [66] V. V. Thacker, S. Ghosal, S. Hernández-Ainsa, N. A. Bell, and U. F. Keyser, *Applied physics letters* **101**, 223704 (2012).
- [67] J. Mathé, A. Aksimentiev, D. R. Nelson, K. Schulten, and A. Meller, *Proceedings of the National Academy of Sciences* **102**, 12377 (2005).
- [68] N. Nikoofard, H. Khalilian, and H. Fazli, *The Journal of Chemical Physics* **139**, 074901 (2013).
- [69] N. Nikoofard and H. Fazli, *Soft Matter* **11**, 4879 (2015).
- [70] L.-Z. Sun, H. Li, X. Xu, and M.-B. Luo, *Journal of Physics: Condensed Matter* **30**, 495101 (2018).
- [71] B. Tu, S. Bai, B. Lu, and Q. Fang, *Scientific reports* **8**, 1 (2018).
- [72] A. Nikolaev and M. E. Gracheva, *Nanotechnology* **22**, 165202 (2011).